055 **MULTI-SCALE COMPRESSION-BASED QUANTITATIVE ELASTOGRAPHY AND ITS APPLICATION TO BLOOD PRESSURE ESTIMATION.**

AM Zakrzewski[1], SY Sun[1], MW Gilbertson[1], B Vannah[1], L Chai[1], J Ramos[1], BW Anthony[1].*

[1]Massachusetts Institute of Technology, Cambridge, MA, USA.

Submitted for publication in final form: October 2, 2012.

Abstract

Compression-based ultrasonic quantitative elastography is implemented using a coarse-to-fine multi-scale approach. The multi-scale approach, tested in simulation and on phantoms, results in a 5 % decrease in required computational time to reconstruct accurately the tissue stiffness. The methods are extended to estimate, in simulation, blood pressure and arterial wall stiffness in addition to bulk tissue stiffness. Results show that pressure and vessel stiffness are accurately estimated to within 10 % error.

I. Introduction

Elastography is a method that uses an imaging modality to measure the elastic properties of soft biological tissue. It gives doctors the ability to diagnosis breast cancer because cancerous tumors have a higher elastic modulus than surrounding healthy tissue. Since its introduction in 1991 by Ophir [1], elastography has been developed and refined into a useful medical tool for doctors. The concepts of elastography have been applied to a number of imaging modalities - magnetic resonance imaging, computed tomography, shear wave ultrasound, and compression-based ultrasound - using either a quasi-static or a transient approach. The current methods of quantitative elastography are accurate, but can be made faster by using different computational techniques.

To the authors' knowledge, no group has published research that uses elastography to measure quantitatively the elastic properties of the arterial wall or the pressure within a blood vessel. While blood pressure is currently obtained using sphygmomanometers and invasive catheters, the former cuts off blood flow and causes bruising while the latter risks infection, bleeding, and blood clots. Information about the arterial wall and a non-invasive, potentially continuous way to measure blood pressure could improve doctor's ability to diagnose problems.

This paper focuses on quasi-static compression-based ultrasound elastography. A multi-scale approach is used, which makes the current algorithms even faster. The paper also suggests a noninvasive, continuous elastography-based method to estimate blood pressure and arterial wall stiffness. It is divided into a study that applies a multi-scale approach to the traditional elastography problem, which is validated both in simulation and in phantoms, and into a simulation study concerning blood pressure and arterial wall stiffness estimation.

II. Methods

A. Traditional Elastography Problem

In order to simulate the traditional elastography problem, Field II was used to form B-Mode images [2, 3] and a course-to-fine cross-correlation technique was used to estimate displacement and strain from these B-Mode images [4]. The elastography inverse problem was solved in Matlab (Mathworks, Natick, MA, USA) with calls to the commercial finite element program Abaqus (Dassault Systemes, Providence, RI, USA). Linear displacement-based plane strain quadrilateral elements were used to discretize biological tissue. The tissue was modeled as materially linear elastic with a Poisson ratio of 0.495 and the problem was assumed to be geometrically nonlinear. During the inversion, the known pressure was applied to the top of the simulated tissue and axial displacement boundary conditions were applied to the remaining three sides of the tissue.

The inverse problem is defined as the minimization of the objective function,

$$f = 0.5\,(u_c - u_{known})^T(u_c - u_{known}), \quad (1)$$

where u_{known} is a vector of the displacements measured using the cross-correlation technique, while u_c is a vector of displacements that the algorithm predicts. To solve the minimization problem, the Levenberg-

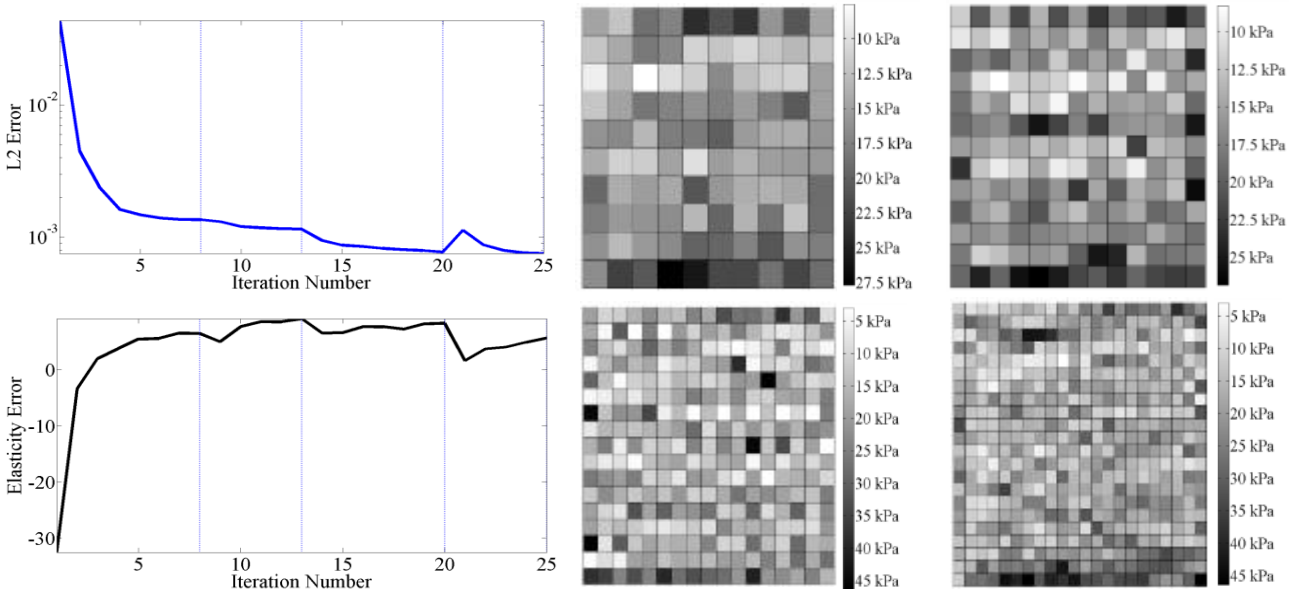

Fig. 1: Elastography performed on a uniform, simulated phantom. Clockwise from top left: the L_2 error of the displacements, the elastography solution on the first coarse mesh, on the 2nd mesh, the 4th mesh, the 3rd mesh, and a plot of the percent error for the elasticity versus iteration number.

Marquardt nonlinear optimization scheme with trust regions was used and the optimization step is defined by

$$\Delta x = x - (J^T J + \mu I)^{-1}\big(J^T(u_c - u_{known})\big), \tag{2}$$

where, for n elements and m nodes, J is the Jacobian matrix of size m×n, I is the identity matrix of size n×n, μ is the scalar damping parameter, u_c and u_{known} are defined as above with size m×1, x is a n×1 vector containing the elastic modulus of each finite element, and Δx is the n×1 vector containing the optimization step [5, 6]. The damping parameter μ is varied during each iteration in order to obtain the largest step possible without sacrificing accuracy. The elasticity of each soft tissue finite element is restricted to be between 0 kPa and 300 kPa, while the step size, Δx, is also restricted in order to prevent overstepping. Smoothing was used after each iteration, as suggested by [7], using the equation

$$x_n = (1-\theta)x_i + \theta \sum_{j=1}^{r} \left(\frac{1}{r-1}\right) x_{ij}, \tag{3}$$

where θ is the smoothing parameter, x_i is the elastic modulus of element i, r is the number of elements adjacent to element i, x_n is the smoothed elastic modulus for element i, and x_{ij} is the elastic modulus of the j^{th} element adjacent to element i. For this paper, the smoothing parameter was set to 0.3.

To solve this elastography problem, a multi-scale approach is used. In this approach, the inverse problem is initially solved on a coarse mesh, and the solution is interpolated onto an increasingly finer mesh. Thus, the resolution of the elasticity distribution increases with every new mesh. This process is demonstrated in Fig. 1 for a uniform simulated phantom, where the upper left hand mesh is the initial coarse mesh. The mesh automatically refines when the objective function changes by less than 1% over successive iterations.

This multi-scale approach is better than many existing methods. Using the solution of the inverse problem on coarse meshes as an initial guess on increasingly finer meshes reduces the number of iterations (and thus the number of Jacobian calculations) that need to be completed to solve the problem with high resolution. This is especially important because the Jacobian calculation is the slowest part of the algorithm. The reduction of iterations using high-resolution finite element meshes is compounded with the fact that the finite element model runs much more quickly for coarse meshes. In a clinical real-time application of elastography, these considerations might be important.

The validity of the elastography approach described above was confirmed on experimental phantoms made of a mixture of mineral oil and styrene-ethylene/butylene-styrene (SEBS) copolymer [8]. A Terason 3000t system (Teratech, Burlington, MA, USA) collected radio frequency data, using the Terason software development kit (SDK), for subsequent displacement estimation. For these experiments, an acrylic compression plate is used in order to eliminate edge effects by ensuring uniform applied pressure on the top of the phantom. The applied force during tissue displacement was measured using a 3D printed probe attachment that connects to a force gauge [9], see Fig 2. This robust and accurate measure of force is

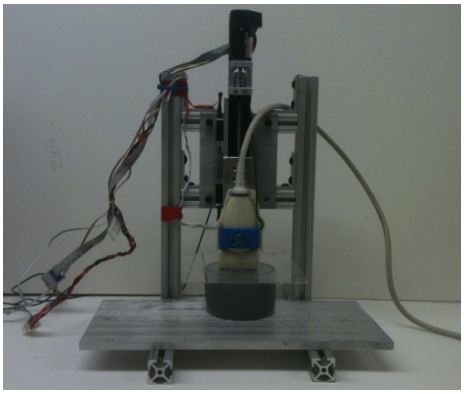

Fig. 2: Experimental setup showing the force measurement probe attachment.

critical to obtaining a quantitative estimation of tissue elasticity without any need for further assumptions.

B. Blood Pressure and Arterial Wall Stiffness Problem

The algorithms described above are applied to measure, in simulation, blood pressure and arterial wall stiffness. In this problem, it is assumed that the arterial wall and blood pressure do not have an angular dependence. Vessels are assumed to be circular in cross-section and are assumed to be plaque free. The blood is modeled as a pressure boundary condition and the arterial wall is modeled using linear truss elements. Truss elements are used for three reasons. First, circumferential stiffness, as opposed to bending stiffness, governs the behavior of the vessel and this behavior is well reflected in the assumptions made in the truss element formulation. Second, a sufficiently fine quadrilateral mesh for the arterial wall would greatly increase computational time because of mesh size transition requirements between the arterial wall and bulk tissue. Third, and most importantly, the displacements of the arterial wall obtained with linear truss elements agree very well with the displacements obtained using plane strain elements, which have been previously used to model the arterial wall [10]. The arterial wall elements share nodes with the bulk plane strain elements so that the displacements of the arterial wall exactly equal that of the soft tissue that connects to it.

Quadrilateral mesh generation is completed automatically in Matlab by writing a rectilinear grid, removing elements to make space for the vessel, then projecting nodes that are near the vessel onto the vessel surface. In order to obtain a good mesh using this technique, quadrilateral mesh smoothing algorithms, as described in [11], are applied in order to optimize the internal angles of each element, promote uniformity among element edge length, and force elements on the tissue's boundary to have edges as perpendicular as possible to the boundary.

The objective function used to solve the inverse problem is still that of Eq. (1) above. However, the wall stiffness and pressure are each treated as a variable to be optimized. Thus, the optimization step changes to

$$\Delta v = v - (J^T J + \mu I)^{-1}\left(J^T (u_c - u_{known})\right), \tag{4}$$

where v=[x;p;a], a is the arterial wall stiffness and p is the blood pressure. The Jacobian matrix is now of size m×(n+2) and the identity matrix, I, becomes a (n+2)×(n+2) matrix.

The blood pressure and arterial wall stiffness are highly coupled in this problem. In order to stabilize the solution and ensure convergence to the known values of pressure and arterial wall stiffness, four image pairs are obtained and used in the inversion process. Using the four image pairs, the number of nodes in u_c and u_{known} are multiplied by 4, but the number of variables to optimize remains fixed at n+2.

III. Results and Discussion

A. Traditional Elastography Problem

Applying the algorithms described above, there is excellent agreement between the known elastic modulus and the elastic modulus predicted by the program. In Fig. 3, the elasticity distribution is shown for a simulated inclusion. The elastography region of interest is 40 mm by 40 mm and the inclusion has a diameter of 10 mm. The bulk tissue has a true elastic modulus of 15 kPa while the inclusion has a true elastic modulus of 30 kPa. By-hand segmentation was used to identify the inclusion in the reconstructed elastogram. The mean stiffness of the inclusion and the mean stiffness of the bulk material are accurately

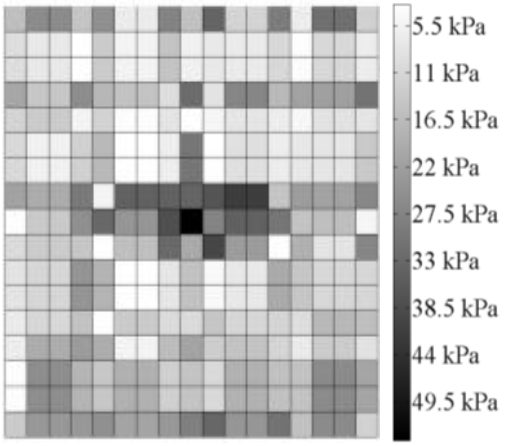

Fig. 3: Elasticity distribution of a simulated phantom with an inclusion.

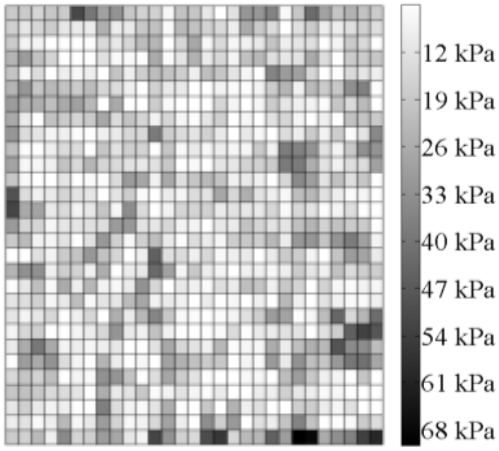

Fig. 4: Elasticity distribution of a co-polymer and mineral oil phantom.

reconstructed to less than 5 % error. The signal to noise ratio for this problem is defined as

$$SNR = \frac{s}{\sigma}, \tag{5}$$

where s is the mean elasticity of the region of interest and σ is the standard deviation. For this simulated inclusion, the SNR is equal to 1.8 within the bulk tissue and 1.9 within the inclusion. The contrast transfer efficiency can be defined by

$$\gamma = |C_E(dB)| - |C_T(dB)|, \tag{6}$$

where C_E is the elasticity contrast obtained from elastography and C_T is the true elasticity contrast. For this simulated inclusion model, γ is 0.12.

Because the specific time of each iteration is misleading due to significant overhead in Abaqus calls, the advantages of the multi-scale approach are expressed as a percentage decrease in computational time. Comparing the multi-scale approach to the non-multi-scale approach when fine resolution elastograms are required, there is a 5 % computational resource improvement. Further, an accurate elasticity reconstruction of the tissue can be obtained in 10 iterations on a coarse mesh.

Applying this algorithm to experimental phantoms, the results show an accurately reconstructed elastic modulus to less than 5 % error as well. In Fig. 4, the elastic modulus distribution is shown for a uniform phantom, whose known elastic modulus is 16.5 kPa, obtained from compression tests. The signal to noise ratio of the reconstruction is 1.48.

B. Blood Pressure and Arterial Wall Stiffness Problem

As with the material properties used for the traditional elastography problem, the material properties of the vessel simulations were motivated by clinically relevant values; the arterial wall stiffness, soft tissue stiffness, and blood pressure were 400 kPa, 15 kPa, and 10 kPa (approximately 80 mmHg), respectively. As described in the methods section, four image pairs are used to stabilize the vessel problem. Compressions

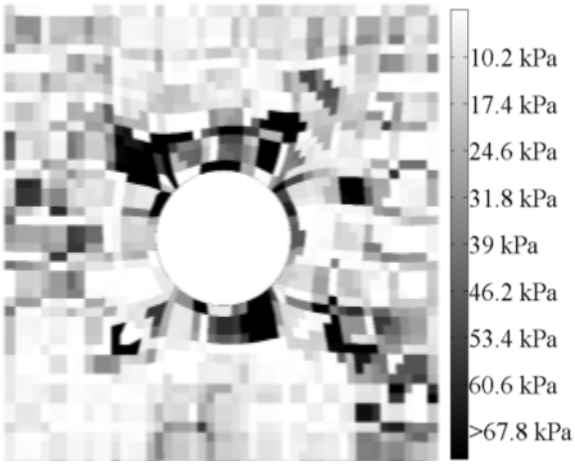

Fig. 5: Elasticity distribution of blood pressure and arterial wall simulation.

of 1%, 2%, 3%, and 4% of the total axial dimension of the simulated phantom were used as input into the elastography algorithm. The elastography region of interest was 40 mm by 40 mm while the vessel had a diameter of 10 mm.

In Fig. 5, the elastic modulus distribution of the bulk tissue is shown. The resulting bulk elastic modulus, blood pressure, and wall stiffness are reconstructed to within 10 % of the known values. The signal to noise ratio, defined as discussed above, is 0.54.

IV. Conclusions

To the authors' knowledge, compression-based ultrasound elastography has not been applied to measure blood pressure and arterial wall stiffness. This paper demonstrates the feasibility of such measurements and demonstrates computational improvements over the traditional elastography solution by using a multi-scale approach.

Future work on the estimation of arterial wall stiffness and blood pressure using elastography methods should focus on increasing the stability of the problem with respect to the coupling between the blood pressure and arterial wall stiffness. With better stabilization techniques, the algorithms will be able to reconstruct the arterial wall thickness as well as the quantitative properties of vessel plaque.

The focus of a future paper will concern the implementation of blood pressure and arterial wall stiffness estimation on phantoms as well as comparing the blood pressure elastography measurements in vivo to that obtained using a sphygmomanometer.

Acknowledgements

The authors gratefully acknowledge Kai Thomenius for advice on how to improve this work as well as GE Global Research for funding this research.

References

[1] Ophir J, Cespedes I, Ponnekanti H, Yazdi Y, and Li X (**1991**). "Elastography: A quantitative method for imaging the elasticity of biological tissues," Ultrasonic Imaging, 13, 111-134.
[2] Jensen JA (**1996**). "Field: A program for simulating ultrasound systems," Med. and Biol. Eng. and Comp., 34, 351-353.
[3] Jensen JA, and Svendsen NB (**1992**). "Calculation of pressure fields from arbitrarily shaped, apodized, and excited ultrasound transducers," IEEE Trans. Ultrason., Ferroelec., Freq. Contr., 39, 262-267.
[4] Sun SY (**2009**). *Deformation correction in ultrasound imaging in an elastography framework*, Massachusetts Institute of Technology.
[5] Han L, Noble JA, and Burcher M (**2002**). "The elastic reconstruction of soft tissue," IEEE Int. Symp. Biomed. Imag., 1035-1038.
[6] Nielsen H (**1999**). "Damping parameter in Marquardt's method," Technical Report IMM-REP-1999-05, Technical University of Denmark.
[7] Doyley MM, Meaney PM, and Bamber JC (**2000**). "Evaluation of an iterative reconstruction method for quantitative elastography," Phys. Med. Biol., 45, 1521-1540.
[8] Oudry J, Bastard C, Miette V, Willinger R, Sandrin L (**2009**). "Copolymer-in-oil phantom materials for elastography," Ultrasound in Med Biol., 35, 1185–1197.
[9] Gilbertson MW (**2010**). *Handheld force-controlled ultrasound probe*, Massachusetts Institute of Technology.
[10] Baldewsing RA, de Korte CL, Schaar JA, Mastik F, and van der Steen AFW (**2004**). "A finite element model for performing intravascular ultrasound elastography of human atherosclerotic coronary arteries," Ultrasound in Med. Biol., 30, 803-813.
[11] Blacker TD, and Stephenson MB (**1991**). "Paving: A new approach to automated quadrilateral mesh generation," Int. Journal for Num. Methods in Eng., 32, 811-847.